JAAS

Accepted Manuscript

This article can be cited before page numbers have been issued, to do this please use: S. J. Romaniello, M. P. Field, H. B. Smith, G. W. Gordon, M. H. Kim and A. D. Anbar, *J. Anal. At. Spectrom.*, 2015, DOI: 10.1039/C5JA00205B.

ROYAL SOCIETY OF CHEMISTRY

www.rsc.org/jaas

JAAS

PAPER

Fully automated chromatographic purification of Sr and Ca for isotopic analysis

Cite this: DOI: 10.1039/c5ja00205b

S. J. Romaniello,[a] M. P. Field,[b] H. B. Smith,[a] G. W. Gordon,[a] M. H. Kim[b] and A. D. Anbar[ac]

Received 31st May 2015
Accepted 3rd August 2015

DOI: 10.1039/c5ja00205b

www.rsc.org/jaas

We present a commercially-available, fully-automated, offline chromatography method capable of simultaneously purifying both Ca and Sr for stable and radiogenic isotope analysis. The method features effective purification and mutual separation of Ca and Sr from multiple complex matrixes using a single, highly-reusable chromatographic column. Low carryover combined with high yield for multiple extractions indicate the column can be reused for at least 200 samples. Accurate and precise stable and radiogenic data are presented for the USGS standard BCR-2 basalt, NIST-1400 bone ash, IAPSO seawater, and an in-house llama bone standard (CUE-0001). The Sr–Ca method was designed to accommodate a wide variety of sample types, including carbonates, bones, and teeth; silicate rocks and sediments; fresh and marine waters; and biological samples such as blood and urine. The system is highly adaptable and capable of unattended processing up to 60 samples per run at a rate of 32 samples per day on a single chromatographic column.

Introduction

High throughput methods for sample purification are required to effectively exploit new opportunities in the study of radiogenic and non-traditional stable isotopes. Many isotope studies in geochemistry, anthropology, biomedicine and forensics would benefit from larger data sets, but these are often impractical with manual drip chromatography techniques, which can be time-consuming and demand the attention of skilled laboratory staff. Automated methods have been successfully adopted in other fields of isotope studies, including continuous-flow gas-source isotope ratio mass spectrometry and noble gas mass spectrometry.[1,2] Development and adoption of similar approaches for radiogenic and non-traditional stable isotopes has been slower, hindered by the requirement for very low sample carryover and the materials challenge of working with concentrated strong acids.

Applications for Ca and Sr isotopic analysis, including paleoceanography, isotope stratigraphy and sedimentology, isotope forensics, and anthropology are driving a demand for large Ca and Sr isotope datasets.[3–13] Moreover, emerging applications for stable isotope fractionation of metals, such as Ca, are poised to dramatically alter the field.[14–19] Large-scale clinic trials for medical applications of Ca isotopes will require increased sample throughput, rapid turnaround time, and reduced analytical costs—all of which point toward the need for automation. There have been multiple efforts to automate the chromatographic purification of Ca and Sr, including both online and offline methods.[20–25] Although individually successful, these methods have not enjoyed widespread adoption. We believe this is because the proposed approaches often required substantial modification of commercially available hardware, only functioned for a subset of potential sample types, and/or were perceived as analytically inferior to established manual techniques.

The main barriers to automation of Ca and Sr chromatography are the requirements for low blanks and negligible sample carryover, particularly due to the large natural isotope range for radiogenic Sr isotopes. Furthermore, Ca and Sr should be mutually separated both from each other as well as sample matrix for analysis on higher throughput MC-ICP-MS instruments. Eichrom SrSpec™ resin is commonly used both to purify Sr and to remove traces of Sr from Ca samples before isotopic analysis.[26–31] However, SrSpec™ is difficult to repeatedly reuse without extensive cleaning due to a tendency to retain ~0.01–1% of Sr as sample carryover.[27,32]

Here we present a novel fully-automated, offline Ca and Sr separation method which attempts to circumvent the aforementioned difficulties. The method exploits a commercially-available hardware platform and a novel, highly-reusable Sr–Ca column. The analytical performance of this method is evaluated for a range of representative sample matrixes.

[a]School of Earth & Space Exploration, Arizona State University, Tempe, AZ, USA
[b]Elemental Scientific, Inc., Omaha, NE, USA
[c]Department of Chemistry & Biochemistry, Arizona State University, Tempe, AZ, USA

Experimental

Reagents and materials

All reagents used in the sample digestion and separation chemistry are prepared from high purity hydrochloric acid, nitric acid, hydrogen peroxide, and hydrofluoric acid. HCl and HNO_3 were prepared by sub-boiling distillation at ASU. H_2O_2 and HF were Fluka TraceSelect Ultra grade (Sigma-Aldrich, St. Louis, Missouri, USA). Solutions were prepared by dilution with 18.2 MΩ cm deionized water (Table 1).

All materials used for sample handling are made of fluoropolymer, polypropylene or polyethylene, and were acid washed for >24 hours each in 20 vol% HNO_3 and 20 vol% HCl prior to use.

Samples

Chemical purification of Ca and Sr was tested on a variety of sample types including seawater (IAPSO), basalt (BCR-2), bone ash (NIST-1400), and an in-house llama bone standard (CUE-0001). Samples were chosen to span a range of matrix types, Ca/Sr ratios (110, 320, 3350, and 560 mol : mol, respectively) and to provide an intentionally wide range of stable Ca, stable Sr, and radiogenic $^{87}Sr/^{86}Sr$ ratios for the purposes of testing sample carryover.

Digestion and sample dissolution

15 mL of seawater and 100 mg each of bone ash and bone standards were digested on a hot plate using 5 mL of concentrated HNO_3 in Savillex™ PFA vials. Vials were sealed and heated overnight on a hot plate at 110 °C, then evaporated to dryness. Any residual organic residue was digested by heating for several hours at 110 °C in 0.5 mL concentrated HNO_3 + 0.2 mL 30% H_2O_2. The BCR-2 basalt standard (100 mg) was dissolved using 5 mL of HNO_3 and 1 mL of concentrated HF in a sealed Savillex™ PFA vial. The sample was ultrasonicated for 30 minutes and then heated at 110 °C overnight on a hotplate. Following this, 90% of the solution was evaporated and 5 mL of concentrated HCl was added. This solution was heated for several hours to dissolve any residual fluorides. All samples were dried down and dissolved in 2 M HNO_3 in preparation for column chemistry.

Ca and Sr separation

The automated purification of Ca and Sr for isotopic analysis is performed using the prep*FAST* MC (ESI, Omaha, NE, USA) and the supplied 1 mL Sr–Ca column (Part number CF-MC-SrCa-1000). The prep*FAST* MC is a fully-automated, low pressure (<100 psi), fluoropolymer chromatography system that performs several basic functions to isolate elements of interest. It consists of an autosampler, two 6-port 2-position valves, one 10-port multi position valve, a S400V syringe pump with a fill-dispense valve, and a 13 mL sample loop.

The system's integrated software is programmed to perform various functions required for matrix removal and sample purification including column pre-cleaning, column conditioning, sample loading, and matrix and analyte elution and collection. The software allows the user to define the location, volume, flow rate, and destination for each sample and reagent. The software also includes an option to automatically generate sample elution curves by dispensing small reagent increments into user-pre-defined tubes (column calibration mode) or collect cuts in their entirety for normal sample processing.

A description of the column elution protocol used in this study is provided in Table 1. Elution with 2 M HNO_3 + 1 wt% H_2O_2 removes most major and trace matrix elements. Sr is eluted in 6 M HNO_3 and Ca with 12 M HNO_3. In the final step, 10 mL of 1 M HF is used to remove all remaining elements on the resin (REEs, HF, Cd, and U) leaving the resin clean for the next sample. The entire automated protocol requires 45 minutes per sample, allowing 32 samples to be processed per 24 hours.

Table 1 Chromatographic steps for the automated separation of Ca and Sr (1 mL ESI Sr–Ca column)

Step	Purpose	Volume	Reagent
1	Condition column	10 mL	2 M HNO_3 + 1% wt H_2O_2
2	Load sample	1 mL	2 M HNO_3
3	Elute sample matrix	10 mL	2 M HNO_3 + 1% wt H_2O_2
4	Elute Sr	10 mL	6 M HNO_3
5	Elute Ca	10 mL	12 M HNO_3
6	Elute REEs, Hf, Cd, U	10 mL	1 M HF

Elemental concentrations

Blanks and yields were measured on a ICAP-Q quadrapole inductively-coupled plasma mass spectrometer (Thermo Scientific, Bremen, Germany) at Arizona State University. Samples were analyzed in 0.32 M HNO_3 and quantified using a multielement internal standard in combination with external calibration curves. Doubly-charged Sr ($^{84}Sr^{++}$, $^{86}Sr^{++}$, $^{88}Sr^{++}$) represents a significant interference on $^{42}Ca^{+}$, $^{43}Ca^{+}$, and $^{44}Ca^{+}$, which was corrected by measuring $^{87}Sr^{++}$ at mass 43.5 amu in high-resolution mode and assuming an $^{87}Sr/^{86}Sr$ ratio of 0.71.

Ca and Sr isotopic measurements

Ca and Sr isotopic compositions were measured at Arizona State University using a Neptune multi-collector inductively-coupled plasma mass spectrometer (MC-ICP-MS, Thermo Scientific, Bremen, Germany) equipped with a Jet sample cone, an H-skimmer cone, and an Apex-Q desolvating nebulizer (ESI, Omaha, NE, USA).

Ca isotope measurements were performed using sample-standard bracketing in medium resolution following previous published methods.[16,30,33] Optimized instrument operating parameters were sample gas = 0.9 L min^{-1}, auxiliary gas = 0.9 L min^{-1}, cool gas = 14.50 L min^{-1}, N_2 = 2–5 mL min^{-1}. Ca samples were introduced at a concentration of 3 ppm and flow rate of 200 μL min^{-1}, yielding a sensitivity of ~3.3 V $^{44}Ca^{+}$ per ppm Ca. Samples were introduced in a matrix of 0.16 M HNO_3 which eliminates nebulizer clogging associated with the formation of $CaNO_3$ precipitates when using a higher concentration HNO_3 matrix. Faraday cups were positioned to collect $^{42}Ca^{+}$, $^{43}Ca^{+}$, $^{44}Ca^{+}$, $^{45}Sc^{+}$, $^{47}Ti^{+}$, and $^{48}Ca^{+}$. The Ca and Ti

positions were offset relative to $^{45}Sc^+$, aligning the peak center of $^{45}Sc^+$ on the center cup with the uninterfered low-mass shoulder of the Ca and Ti isotopes.[33] In medium resolution, the typical width of the uninterfered low-mass shoulder was 0.004 amu and the optimal peak position was determined by systematically measuring the standard deviation of the Ca isotopic ratios at 0.001 amu intervals across the peak shoulder. Each measurement consisted of 25 8.4 s cycles. Samples were measured relative to an in-house ICP Ca solution (ICP1; NIST 10 000 ppm ICP Ca standard, lot #X-10-39A) and converted to the SRM915a scale by subtracting $\delta^{44/42}Ca = -0.25 \pm 0.01‰$ (2se, $N = 188$).[30] Data quality and precision was assessed by measuring each sample 3 times as well as intercomparison of the $\delta^{44/42}Ca$, $\delta^{44/43}Ca$, $\delta^{48/42}Ca$ on a per amu basis. Final data are reported on as $\delta^{44/42}Ca_{SRM915a}$ with a typical 2σ precision of 0.06‰.

Radiogenic ($^{87}Sr/^{86}Sr$) and stable ($\delta^{88/86}Sr$) Sr data were obtained simultaneously in low-resolution using sample-standard bracketing with Zr-element doping.[28,29,34] Zr was added to all samples and standards at a concentration of 15 ppb. Sr samples were introduced at 25 ppb and a flow rate of 200 μL min^{-1} in a matrix of 0.32 M HNO_3 yielding a sensitivity of ~0.7 V $^{88}Sr^+$ per ppb Sr. Faraday cups were positioned to collect $^{82}Kr^+$, $^{83}Kr^+$, $^{84}Sr^+$, $^{85}Rb^+$, $^{86}Sr^+$, $^{87}Sr^+$, $^{88}Sr^+$, $^{90}Zr^+$, and $^{91}Zr^+$. Each measurement consisted of 20 8.4 s cycles, and samples were run in blank-standard-sample-standard-blank blocks, with SRM 987 Sr as the bracketing standard. Kr, a trace impurity in high-purity Ar gas, was measured at $^{83}Kr^+$ with a typical intensity of ~280 μV. A first-order correction was performed by subtracting on-peak blank intensities measured every fourth analysis in "blank-std-smpl-std-blank" brackets. This reduced the magnitude of the blank-subtracted ^{83}Kr to ±30 μV. Correction for the residual Kr was made assuming an $^{83}Kr/^{84}Kr$ ratio of 0.201750, an $^{83}Kr/^{86}Kr$ ratio of 0.664533, and an exponential mass bias correction based on an $^{86}Sr/^{88}Sr$ ratio of 0.1194. A Rb correction was applied similarly, assuming an $^{85}Rb/^{87}Rb$ ratio of 2.58896. The typical magnitude of the Kr and Rb correction following subtraction of the on-peak blanks was ~15 ppm on the $^{87}Sr/^{86}Sr$ ratio. Following interference correction, radiogenic Sr was corrected for instrument mass bias by normalizing to $^{86}Sr/^{88}Sr = 0.1194$. Stable Sr values were corrected in two stages by first normalizing all samples and standards to a constant $^{91}Zr/^{90}Zr$ ratio followed by sample-standard bracketing. Each sample was measured 3 times, with a typical 2σ precision of 0.00001 for $^{87}Sr/^{86}Sr$ and 0.04‰ for $\delta^{88/86}Sr$.

Results and discussion

Ca and Sr elution

High precision isotopic analyses of Ca and Sr by MC-ICP-MS can be affected by a number of isobaric and matrix interferences summarized in Table 2. The most important direct isobaric interferences for Ca include $^{48}Ti^+$ on $^{48}Ca^+$, doubly-charged $^{84,86,88}Sr^{++}$ on $^{42,43,44}Ca^+$, respectively, and gas-derived interferences such as $^{14}N_3^+$, $^{12}C^{16}O_2^+$, and $^{14}N_2{}^{16}O^+$.[30,31,33] The most important isobaric interferences for Sr include $^{87}Rb^+$ on $^{87}Sr^+$, gas-derived $^{84,86}Kr^+$ on $^{84,86}Sr^+$, and sample-derived Zr which interferes with the Zr-doping procedure commonly used to correct instrument mass bias for stable Sr isotope measurements.[35] Both Ca and Sr stable isotope measurements are also subject to matrix interferences resulting from variations in instrument mass bias due to variable sample ionic strength.[30] As a result, major matrix elements such as Na, Mg, K, and Fe must be separated from Ca and Sr prior to analysis.

The Sr–Ca column allows direct separation of Ca and Sr from complex sample matrices using a single column. Fig. 1 shows elutions curves for each standard used in this study. These curves were generated automatically, using the column calibration feature of the prep*FAST*-MC. The first step efficiently removes most matrix elements including Na, Mg, Al, K, Ti, Fe, Rb, Zr, and Ba in 2 M HNO_3. This is followed by elution of Sr and Ca in 6 M and 12 M HNO_3, respectively. Previous studies have shown that doubly-charged Sr is a potentially significant interference on MC-ICP-MS measurements of Ca isotopes and requires a Ca/Sr ratio >10 000 to avoid significant analytical artifacts.[30] This method allows for consistent separation of Sr from Ca with a Ca/Sr ratio greater than 100 000 (Table 3). The remaining retained elements, including rare earths, Cd, Zr, and U are discarded from the column in the final wash column step using 1 M HF. The purity of the BCR-2 Sr and Ca elution cuts are tabulated as Ca and Sr/elemental ratios before and after separation (Table 3).

Column yield and lifespan

The capability to reuse the column for multiple samples is crucial in determining the length of automated runs. Percent yields for Ca and Sr are plotted for 60 consecutive samples processed over 48 h (Fig. 2). High constant yields of greater than 93 ± 2% for both Ca and Sr indicate no degradation in binding efficiency for up to 60 extractions. Continued sample processing beyond this experiment did not exhaust the column and our experience suggests that up to 200 samples can be extracted on a single column.

Table 2 Major isobaric and matrix interferences for Ca and Sr isotopes measurements by MC-ICP-MS

	$^{42}Ca^+$	**$^{43}Ca^+$**	**$^{44}Ca^+$**	**$^{48}Ca^+$**
C			$^{12}C^{16}O_2^+$	
N	$^{14}N_3^+$		$^{14}N_2{}^{16}O^+$	
K	$^{41}K^1H^+$			
Ti				$^{48}Ti^+$
Sr	$^{84}Sr^{++}$	$^{86}Sr^{++}$	$^{88}Sr^{++}$	
	$^{84}Sr^+$	**$^{86}Sr^+$**	**$^{87}Sr^+$**	**$^{88}Sr^+$**
Ca	$^{40}Ar^{44}Ca^+$	$^{40}Ar^{46}Ca^+$	$^{43}Ca^{44}Ca^+$	$^{40}Ar^{48}Ca^+$
Rb			$^{87}Rb^+$	
Kr	$^{84}Kr^+$	$^{86}Kr^+$		
	BCR-2	**CUE-0001**	**IAPSO**	**NIST 1400**
Matrix	Al, Fe, Mg	Ca, P	Na, Mg, K	Ca, P

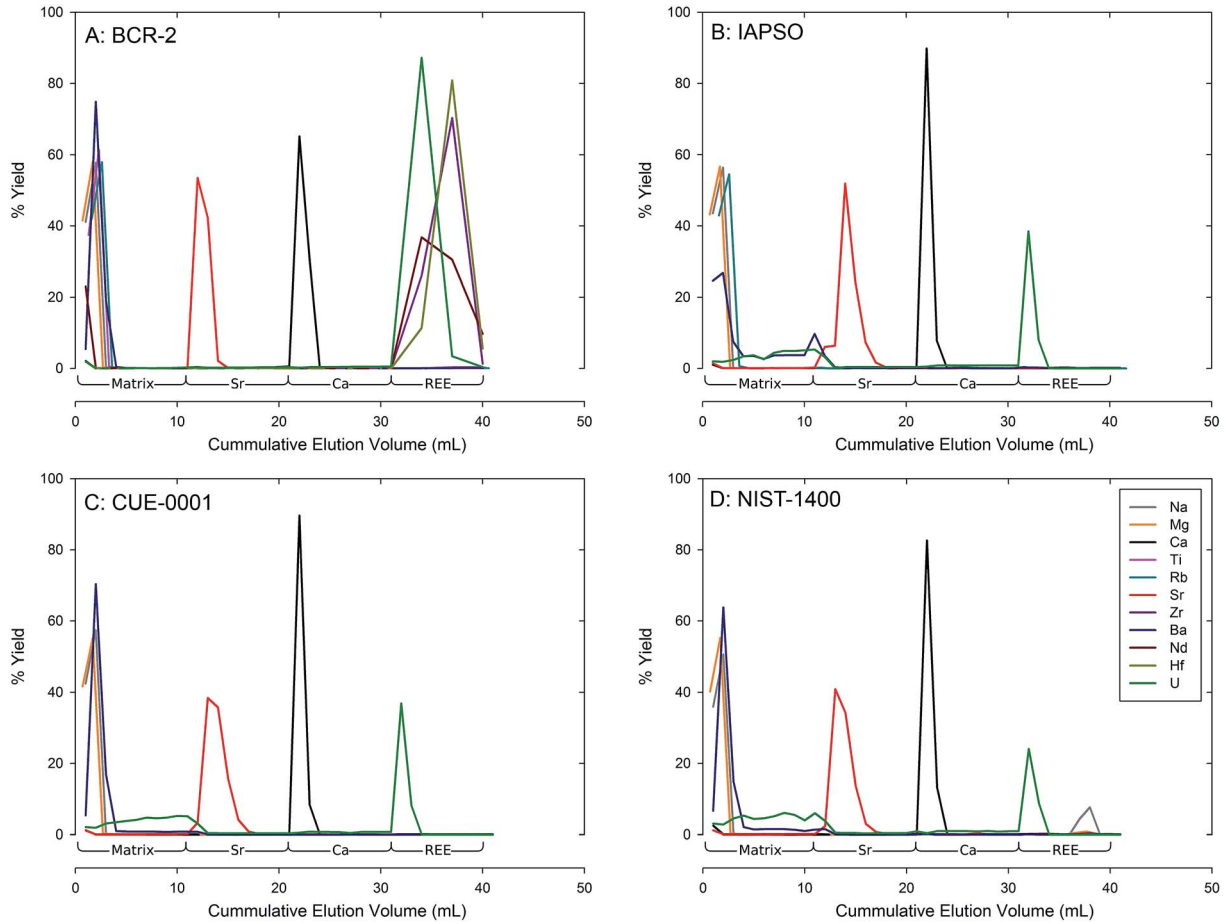

Fig. 1 Elution profiles for BCR-2 basalt (A), IAPSO seawater (B), CUE-0001 llama bone (C), and NIST-1400 bone ash (D). Elution curves were generated automatically using the prep*FAST*-MC column calibration mode. Sample sizes for each standard were ~100 μg Ca, corresponding to 1.9 mg BCR-2, 240 μL IAPSO, 0.26 mg NIST-1400, and 0.50 mg of CUE-0001. Sr and Ca are separated from all major matrix components and potential interferences.

Column capacity

Previous work has shown low chromatographic yields can result in isotopic fractionation of Ca and Sr during purification.[30,36–39] Although the method described here results in nearly quantitative recovery of Ca and Sr, Ca and Sr yields can be negatively impacted if the sample size exceeds the capacity of the resin to bind analyte ions. To determine the column capacity, yields and stable Ca and Sr isotopes were measured as function of sample mass (Fig. 3). The samples consisted of 0.026–2.6 mg of NIST 1400 bone ash (10–1000 μg Ca).

Table 3 Efficiency of chromatographic separation for BCR-2 (1.9 mg BCR-2, 100 μg Ca)

Sr ratios	Before separation	After separation	Improvement factor
Sr/Ca	0.007	0.121	16.4
Sr/Rb	7.17	>2237[a]	>312
Sr/Zr	1.97	1051	535
Ca ratios			
Ca/K	3.26	1735	533
Ca/Ti	3.63	>18 742[a]	>5170
Ca/Sr	136	129 612	955

[a] Interference below limit of detection following purification.

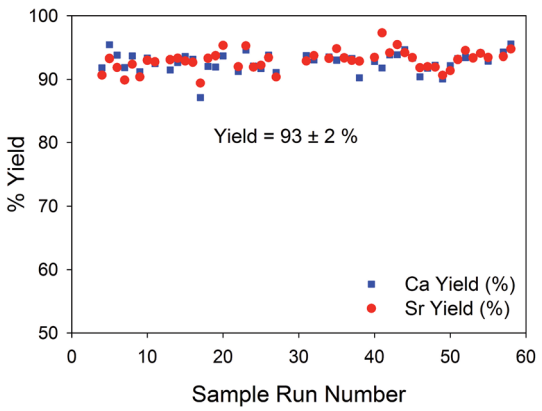

Fig. 2 Recovery of Ca and Sr collected during a typical sample run consisting of 60 limestone, dolostone, coral, and seawater samples.

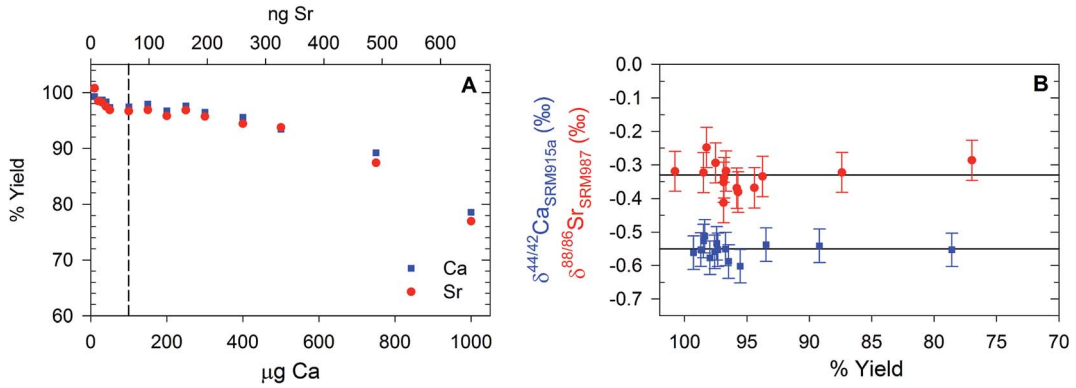

Fig. 3 (A) Recovery of Ca and Sr from NIST 1400 bone ash (Ca/Sr ratio of 1550) plotted as a function of sample mass (μg Ca). The recommend sample size (~100 μg Ca) is represented by the vertical dashed line. (B) Stable Ca ($\delta^{44/42}$Ca) and Sr ($\delta^{88/86}$Sr) isotope composition of NIST 1400 bone ash *versus* recovery of Ca and Sr, respectively. The data demonstrate no measurable stable isotopic fractionation of Ca and Sr on the column even when the column is intentionally saturated with Ca producing yields as low as 75%.

Because Ca is the only major element which binds to the Sr–Ca column during separation, Ca and Sr yields are primarily controlled by the mass of Ca loaded onto the column. Samples up to 300 μg Ca show greater than 95% yield for Sr and Ca. Loading more than 300 μg of Ca on the 1 mL column results in breakthrough and parallel decreases in Ca and Sr yields to approximately 75% at 1000 μg of Ca. Based on these results, a typical sample size of 100 μg Ca is suggested (Fig. 3a).

An interesting feature of the Sr–Ca column is that isotopic fractionation on the column appears to be minimal for both Ca and Sr (Fig. 3b). Even with yields as low as 75%, the measured stable isotopic composition of Ca and Sr in NIST 1400 was indistinguishable from samples with nearly 100% yield at current measurement precision (Fig. 3b).

Blanks and sample carryover

Overall method blanks were determined by processing 2 M HNO_3 blank samples randomly interspersed with samples during a typical run sequence. Measured blanks were similar to conventional Ca and Sr manual drip methods, 100 ng Ca and 30–150 pg Sr, respectively.[27,31,32] Correlation of measured Sr blanks with the total Sr in the previous sample suggests that carryover was limited to a factor of $<4 \times 10^{-5}$. This level of carryover is similar to reagent blanks and results in negligible isotopic shift even for relatively large variations in radiogenic $^{87}Sr/^{86}Sr$ ratios. For example, for similarly-sized samples, the calculated carryover of a radiogenic sample with $^{87}Sr/^{86}Sr = 0.74$ on a sample with $^{87}Sr/^{86}Sr = 0.70$, would represent only a 2.4 ppm error.

Method validation samples

In order to test overall method performance, four samples were chosen to represent a range of sample matrix types with variable Sr/Ca ratios. The samples include three CRMs (USGS BCR-2 basalt, NIST 1400 bone ash, OSIL IAPSO seawater) and one in-house llama bone standard (CUE-0001). These samples were intentionally chosen to span a range of isotopic compositions, particularly for $^{87}Sr/^{86}Sr$, demanding low sample carryover for accurate and precise results. Each sample was analyzed 4–5 times in a randomly ordered sequence, such that any carryover effects of one sample on the next should be evident as increased scatter in the sample precision.

The results of this test suggest that a variety of matrix types can be processed sequentially with high yields and low carryover, allowing accurate and precise Ca and Sr isotopic measurements (Table 4, Fig. 4). Calcium and strontium yields were greater than 95% for all samples, demonstrating near-quantitative recovery for all matrix types (Fig. 4). Radiogenic $^{87}Sr/^{86}Sr$ for replicate sample aliquots are consistent within the long-term reproducibility of the bracketing SRM 987 standard (2sd = 0.000017) demonstrating negligible sample carryover. The accuracy and precision of both Ca and Sr isotopes are similar to published literature values indicating that the automated method produces high-quality data comparable to existing manual methods.

Table 4 Comparison of measured Ca and Sr isotope data with previously published results

	Measured	Reported	Ref.
$\delta^{44/42}Ca_{915a}$ (‰ ± 2σ)			
IAPSO	0.92 ± 0.06	0.93 ± 0.07	30, 33 and 40–42
BCR-2	0.41 ± 0.07	0.47 ± 0.07	41–43
NIST 1400	−0.54 ± 0.05		
CUE-0001	0.83 ± 0.05		
$\delta^{88/86}Sr_{987}$ (‰ ± 2σ)			
IAPSO	0.36 ± 0.03	0.36 ± 0.04	34 and 44
BCR-2	0.22 ± 0.07	0.22 ± 0.02	29
NIST 1400	−0.32 ± 0.03		
CUE-0001	−0.39 ± 0.04	−0.41 ± 0.05	34
$^{87}Sr/^{86}Sr$ (‰ ± 2σ in the last digits)			
IAPSO	0.709187 ± 9	0.709182 ± 4	29
BCR-2	0.705038 ± 9	0.705015 ± 5	29 and 45
NIST-1400	0.713129 ± 19	0.713150 ± 160	20
CUE-0001	0.704455 ± 9		

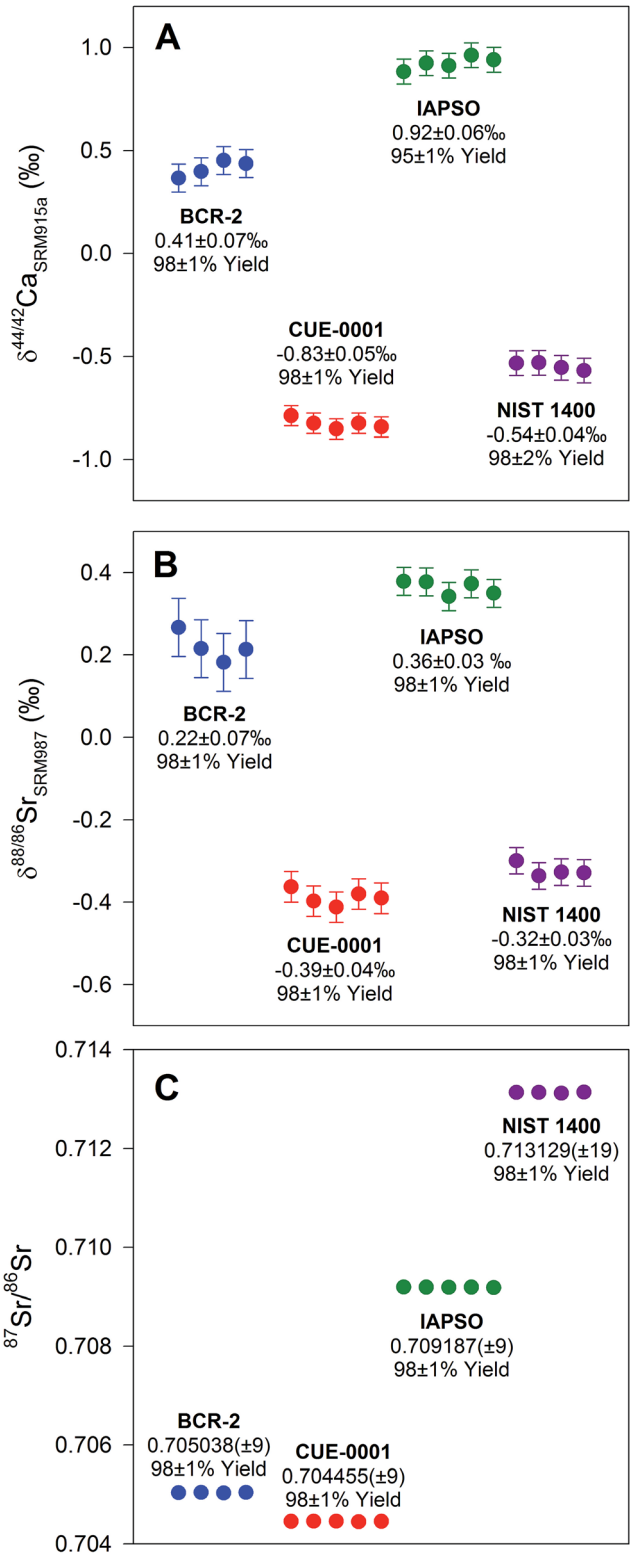

Fig. 4 Reproducibility of Ca and Sr isotope data for a sequence of randomly ordered analyses containing samples of widely varying isotopic compositions. Agreement between replicates demonstrates low system carryover and a high degree of reproducibility.

Conclusion

We present a commercially-available, fully-automated, offline chromatography method capable of purifying both Ca and Sr for stable and radiogenic isotope analysis. This method allows >200 samples to be processed sequentially on the same separation column at a rate of ~32 samples per day.

In addition to increasing sample throughput and reducing personnel costs, automating sample preparation of Ca and Sr for MC-ICP-MS analyses will facilitate acquisition of large, high-resolution data sets and help to expand the use of these isotopic systems in new fields such as biomedical applications of non-traditional stable isotopes.

This method is part of a family of new fully-automated chromatographic methods being developed to address many different isotopic systems including B, Ca, Fe, Cu, Zn, Sr, Cd, Pb, and U using the prep*FAST* MC. These methods are designed to be rugged and transferrable, and to allow the preparation of large, diverse sample sets *via* a highly repeatable process with minimal effort.

Acknowledgements

The authors appreciate Professor Kelly Knudson's permission to use the CUE-0001 standard. Funding support was provided by the NASA Human Research Program (NNX14AB78G), NASA Exobiology Program (NNX13AJ71G), and Elemental Scientific, Inc.

Notes and references

1 J. T. Brenna, T. N. Corso, H. J. Tobias and R. J. Caimi, *Mass Spectrom. Rev.*, 1997, **16**, 227–258.
2 R. H. R. Stanley, B. Baschek, D. E. Lott and W. J. Jenkins, *Geochem., Geophys., Geosyst.*, 2009, **10**, Q05008.
3 R. Alexander Bentley, *J. Archaeol. Meth. Theor.*, 2006, **13**, 135–187.
4 *Isoscapes: Understanding Movement, Pattern and Process on Earth Through Isotope Mapping*, ed. J. B. West, G. J. Bowen, T. E. Dawson and K. P. Tu, Springer, 2010.
5 C. L. Blättler, G. M. Henderson and H. C. Jenkyns, *Geology*, 2012, **40**, 843–846.
6 J. L. Payne, A. V. Turchyn, A. Paytan, D. J. DePaolo, D. J. Lehrmann, M. Yu and J. Wei, *Proc. Natl. Acad. Sci. U. S. A.*, 2010, **107**, 8543–8548.
7 C. L. Blättler and J. A. Higgins, *Geology*, 2014.
8 S. R. Brennan, D. P. Fernandez, G. Mackey, T. E. Cerling, C. P. Bataille, G. J. Bowen and M. J. Wooller, *Chem. Geol.*, 2014, **389**, 167–181.
9 L. A. Chesson, B. J. Tipple, G. N. Mackey, S. A. Hynek, D. P. Fernandez and J. R. Ehleringer, *Ecosphere*, 2012, **3**.
10 M. S. Fantle and E. T. Tipper, *Earth-Sci. Rev.*, 2014, **129**, 148–177.
11 E. M. Griffith, M. S. Fantle, A. Eisenhauer, A. Paytan and T. D. Bullen, *Earth Planet. Sci. Lett.*, 2015, **419**, 81–92.
12 E. M. Griffith, A. Paytan, A. Eisenhauer, T. D. Bullen and E. Thomas, *Geology*, 2011, **39**, 683–686.

13 H. Vollstaedt, A. Eisenhauer, K. Wallmann, F. Boehm, J. Fietzke, V. Liebetrau, A. Krabbenhoeft, J. Farkas, A. Tomasovych, J. Raddatz and J. Veizer, *Geochim. Cosmochim. Acta*, 2014, **128**, 249–265.

14 G. W. Gordon, J. Monge, M. B. Channon, Q. Wu, J. L. Skulan, A. D. Anbar and R. Fonseca, *Leukemia*, 2014, **28**, 2112–2115.

15 A. Heuser and A. Eisenhauer, *Bone*, **46**, 889–896.

16 J. L. L. Morgan, J. L. Skulan, G. W. Gordon, S. J. Romaniello, S. M. Smith and A. D. Anbar, *Proc. Natl. Acad. Sci. U. S. A.*, 2012, **109**, 9989–9994.

17 J. Skulan, T. Bullen, A. D. Anbar, J. E. Puzas, L. Shackelford, A. LeBlanc and S. M. Smith, *Clin. Chem.*, 2007, **53**, 1155–1158.

18 J. Skulan and D. J. DePaolo, *Proc. Natl. Acad. Sci. U. S. A.*, 1999, **96**, 13709–13713.

19 M. B. Channon, G. W. Gordon, J. L. L. Morgan, J. L. Skulan, S. M. Smith and A. D. Anbar, *Bone*, 2015, **77**, 69–74.

20 P. Galler, A. Limbeck, S. F. Boulyga, G. Stingeder, T. Hirata and T. Prohaska, *Anal. Chem.*, 2007, **79**, 5023–5029.

21 S. Garcia-Ruiz, M. Moldovan and J. I. Garcia Alonso, *J. Anal. At. Spectrom.*, 2008, **23**, 84–93.

22 C. Latkoczy, T. Prohaska, M. Watkins, M. Teschler-Nicola and G. Stingeder, *J. Anal. At. Spectrom.*, 2001, **16**, 806–811.

23 P. Galler, A. Limbeck, M. Uveges and T. Prohaska, *J. Anal. At. Spectrom.*, 2008, **23**, 1388–1391.

24 C. L. Blättler, N. R. Miller and J. A. Higgins, *Earth Planet. Sci. Lett.*, 2015, **419**, 32–42.

25 A.-D. Schmitt, S. Gangloff, F. Cobert, D. Lemarchand, P. Stille and F. Chabaux, *J. Anal. At. Spectrom.*, 2009, **24**, 1089–1097.

26 E. P. Horwitz, M. L. Dietz and D. E. Fisher, *Anal. Chem.*, 1991, **63**, 522–525.

27 C. Pin, D. Briot, C. Bassin and F. Poitrasson, *Anal. Chim. Acta*, 1994, **298**, 209–217.

28 L. Yang, C. Peter, U. Panne and R. E. Sturgeon, *J. Anal. At. Spectrom.*, 2008, **23**, 1269–1274.

29 J. Ma, G. Wei, Y. Liu, Z. Ren, Y. Xu and Y. Yang, *Chin. Sci. Bull.*, 2013, **58**, 3111–3118.

30 J. L. L. Morgan, G. W. Gordon, R. C. Arrua, J. L. Skulan, A. D. Anbar and T. D. Bullen, *Anal. Chem.*, 2011, **83**, 6956–6962.

31 T. Tacail, E. Albalat, P. Telouk and V. Balter, *J. Anal. At. Spectrom.*, 2014, **29**, 529–535.

32 C. Pin, A. Gannoun and A. Dupont, *J. Anal. At. Spectrom.*, 2014, **29**, 1858–1870.

33 M. E. Wieser, D. Buhl, C. Bouman and J. Schwieters, *J. Anal. At. Spectrom.*, 2004, **19**, 844–851.

34 K. J. Knudson, H. M. Williams, J. E. Buikstra, P. D. Tomczak, G. W. Gordon and A. D. Anbar, *J. Archaeol. Sci.*, 2010, **37**, 2352–2364.

35 P. Z. Vroon, B. van der Wagt, J. M. Koornneef and G. R. Davies, *Anal. Bioanal. Chem.*, 2008, **390**, 465–476.

36 Y. Fukuda, Y.-H. Zhang, M. Nomura, T. Suzuki, Y. Fujii and T. Oi, *J. Nucl. Sci. Technol.*, 2010, **47**, 176–183.

37 T. Oi, H. Ogino, M. Hosoe and H. Kakihana, *Sep. Sci. Technol.*, 1992, **27**, 631–643.

38 W. A. Russell and D. A. Papanastassiou, *Anal. Chem.*, 1978, **50**, 1151–1154.

39 Y. Fujii, M. Nomura, T. Kaneshiki, Y. Sakuma, T. Suzuki, S. Umehara and T. Kishimoto, *Isot. Environ. Health Stud.*, 2010, **46**, 233–241.

40 D. Hippler, A.-D. Schmitt, N. Gussone, A. Heuser, P. Stille, A. Eisenhauer and T. F. Nägler, *Geostand. Newsl.*, 2003, **27**, 13–19.

41 M. Amini, A. Eisenhauer, F. Böhm, C. Holmden, K. Kreissig, F. Hauff and K. P. Jochum, *Geostand. Geoanal. Res.*, 2009, **33**, 231–247.

42 M. Schiller, C. Paton and M. Bizzarro, *J. Anal. At. Spectrom.*, 2012, **27**, 38–49.

43 F. Wombacher, A. Eisenhauer, A. Heuser and S. Weyer, *J. Anal. At. Spectrom.*, 2009, **24**, 627–636.

44 J. Fietzke and A. Eisenhauer, *Geochem., Geophys., Geosyst.*, 2006, **7**, Q08009.

45 M. S. Fantle, *Geochim. Cosmochim. Acta*, 2015, **148**, 378–401.